v. 3, n. 40, 2023

Journal of
Engineering
Research

ADDITIVE MANUFACTURING BY INSTRUMENTED MASS EXTRUSION

Gustavo Ambone da Silva

João Henrique Araujo Gnoato

Márcia Silva de Araújo

José Alberto Cerri

Abstract: The possibility of creating physical models obtained by additive manufacturing of ceramic mass can contribute to the creative process, cost reduction, increased efficiency of the production process and market acceptance tests for assembling a portfolio. However, the formulation of masses for 3D printing must guarantee cohesion and flowability under pressure, but there is still no established procedure. Observing this opportunity, in order to allow the development of ceramic masses for printing, a three-dimensional movement device was built and tested: a printing table adapted to a universal testing machine, to operate together as an instrumented 3D printer. This device made it possible to study the influence of process parameters, such as mass extrusion speed and movement in the x, y and z axes of the printing table. To this end, force curves were obtained to print the mass versus displacement of the piston in the extrusion. The ceramic mass used was commercial soda earthenware from the company CERMASSA / PASTACER (Campo Largo - PR). The mass for printing has a solid concentration of 73% by mass and plasticity between 3 and 3.4. The extrusion speeds with the best results were 10 and 15% higher than the table movement speed. After sintering, the 2D (one layer) and 3D (three layers) specimens showed good adhesion between the layers and the lowest warpage was obtained when printing in three layers.
Keywords: 3D printing, extrusion, ceramic mass, process parameters, additive manufacturing.

INTRODUCTION

Additive manufacturing enables a series of improvements in the process of creating and developing new products, reducing cost, time and complexity in the process of executing prototypes or models. These parameters directly affect the response time that the ceramic industry has to adjust the demands required by the market. Although 3D printing of polymer test pieces is a standard and commercially accessible procedure, additive manufacturing of 100% ceramic physical models is not yet commercially available in Brazil. An example of the best-known online service for printing polymer prototypes is *i.materialize* [1].

The ISO/ASTM 52900:2021 [2] standard presents the terms and definitions of AM processes, classifying them into seven categories according to the technology used: Binder Jetting (BJT); Direct Energy Deposition (DED); Material Extrusion (MEX); Material Jetting (MJT); Powder Bed Fusion (PBF); Sheet Lamination (SHL), and; Vat Polymerization (VPP). Gibson et al. [3] describe and illustrate each of these processes, dedicating a chapter of the book to each one.

Regarding ceramic materials specifically, Travitzky et al. [4] differentiate the processes according to the size of the layers deposited on top of each other. Figure 1 shows the Additive Manufacturing (AM) processes named according to the ISO/ASTM 52900:2021 standard. However, they are differentiated, as Travitzky et al. [4], with the processes mentioned by the authors included in parentheses.

The direct 3D printing process, in which powder is deposited in suspension to form the 3D part, also called Inkjet Printing, falls under the MJT process [5,6]. In the direct process, the powdered ceramic material can be dispersed in water, organic solvent or wax, and the flow can be continuous, in which the drops

are electrically charged, or discontinuous on demand, in which the drops are generated by pressure [7]. When the vehicle is water, the technique has the advantage of not needing the debinding step to eliminate organic matter from the part before sintering, just drying. Many advanced ceramics have already been manufactured using this technique, such as: SiC, $MoSi_2$, Si_3N_4, PZT, TiO_2 and Al_2O_3, as it offers good precision, as the extrusion nozzles are between 10 and 60 micrometers in diameter. Powders with an average particle size on the nanometric scale are used and, due to the characteristics described, it is considered a one-off manufacture [6], although the concentration of the suspension varies between 20 and 30% by volume of solids [6].

Indirect printing involves dripping or using a spray of a liquid that promotes adhesion between powder particles, which is placed in a reservoir similar to a box, this process being classified as BJT according to Standard [2]. This is considered a one-off impression, made in multiple stages. In the first stage of the BJT process, a uniform and thin layer of powder material is deposited on the printing area, followed by the print head depositing, by means of a jet, the binding material that will adhere only to the particles of the first layer of the straight section of the part to be printed. In the second stage, in some cases, this layer is cured by moving the printing table to the heating region, and then lowering the printing table. This process is repeated until all layers of the part are printed. After printing, the part still goes through the drying, debinding and sintering stages [8]. Commercially, different powder materials can be used in this printing method, such as: alumina, titanium dioxide, tungsten carbide, silica and gypsum [3, 6, 9].

The term Selective Laser Sintering / Melting (SLS/SLM) is more common for ceramic materials than PBF. The SLS process is considered an in-line process, in which the part is obtained by spreading a thin layer of one or more powdered raw materials on the printing table [10]. Then, a computer-controlled laser beam falls on the surface of the raw materials, sintering it and producing the first cross section (2D), in the thickness of the spread layer. Subsequently, the sintered surface is moved downwards in the z axis, followed by the spreading of another layer of raw material and sintering is carried out again by the laser. This operation is repeated until all cross sections (layers) have been sintered, resulting in the three-dimensional constitution of the physical model. At the end of the process, excess non-sintered material is easily removed, as it remains in powder form and can be reused [10, 11]. Some ceramic materials used by this technique are: silica, alumina, composites of silica and alumina or zirconia and yttrium oxide or alumina and zirconia [12].

In the DED process the raw material is in powder form, focused thermal energy is used to fuse or sinter the material as it is being deposited by a head, which differs from the previous system, which is made on a powder bed [3]. Ceramic materials are more difficult to process, as few of them can fuse to form a pool, in addition to suffering thermal shock during cooling, which is why they are more common to be processed into composites, such as Ti/TiC [3]. Lakhdar et al. [6] highlight some ceramic materials processed by this technique, such as: α-Al_2O_3, Al_2O_3–ZrO_2 (Y_2O_3) e Al_2O_3–$Y_3Al_5O_{12}$.

The in-line AM called MEX according to the Standard would correspond to Extrusion Free forming (EFF) [4], other variations would be: Robocasting (RC) [5, 6], Direct Ink Writing (DIW) [6] and Freeze-extrusion Fabrication (FEF) [4, 6]. MEX refers to both the continuous extrusion of a ceramic paste and a material in the form of a filament composed

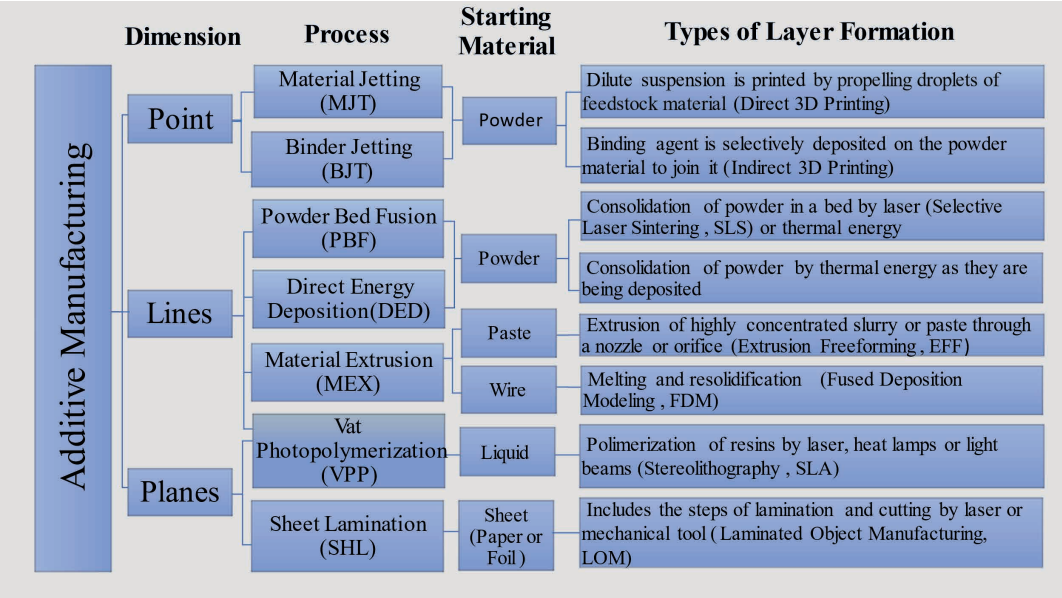

Figure 1: Classification of printing types according to the size of the material deposited layer by layer

of polymeric and ceramic material, which in this case can be called Fused Deposition of Ceramics (FDC) [4] derived from Fused Deposition Modeling (FDM) for composite materials [6]. Plastic ceramic materials such as kaolinete clay [13, 14] and porcelain [15] are produced in paste form by this technique easily, while non-plastic materials such as alumina use carriers or binders [16]. Using this technique, it is possible to obtain parts with high density using a suspension with up to 56% solids by volume [16].

Stereolithography (SLA) is considered the first additive manufacturing technique, developed in 1986 and commercialized by 3D *Systems*. This technique consists of selectively curing a photosensitive liquid resin on the surface [17]. It is also applied to ceramic materials, when it is mixed with resin [3, 4], according to the standard, it would be called Vat Photopolymerization [2]. Some ceramic materials used were: SiO_2, Al_2O_3, ZrO_2 and SiC [17]

The SHL process uses sheets of paper, polymers, metals or ceramics. In the case of ceramic materials, these are in the form of an unsintered green sheet (tape casting or extruded) or in the form of an uncured composite of polymeric resin and ceramic fibers (Prepreg). The overlapping sheets connect under the effect of heat and compression to form a piece [3, 6].

Regarding the number of process steps, it is possible to highlight the processes called PBF and DED, which have the advantage of being processes in a single step, without subsequent drying and debinding, densification occurs during printing. While all others are in multiple stages [6].

The potential and opportunities of AM processes were presented by Zocca et al. [18], who understand that AM processes are more suitable for the production of porous parts, but that obtaining dense parts with surface quality is more successful when the feedstock is based on liquids or pastes, rather than on solid material in dust. Among those that use liquid or paste, only the MJT, DED and MEX techniques are direct processes, that is, without the need to remove excess material. However, MEX printers with the initial raw material in paste or filament are simpler and cheaper solutions than other methods [18].

Therefore, MEX has been used to produce

clay-based materials, as there are several low-cost commercial equipment in one or two steps, in which the extruder can contain a pneumatic or mechanical piston [14]. Thus, the 3D extrusion printing manufacturing technique can constitute a competitive advantage for ceramic companies in the traditional ceramics sector, as highlighted by Costa et al [19]. The difference is based both on the development of prototypes produced with the same raw material as the final piece, and on the production of exclusive and/or customized pieces. These actions have the potential to promote a rapid update of portfolios that allow market demands to be met, thus constituting an innovation for companies in this sector.

In order to allow the construction of low-cost machines, which can be commercialized for large-scale production, it is necessary to understand the process parameters. To this end, this work proposed the construction of an adaptable device in a universal testing machine to help define these quality parameters for each type of dough. In the construction of this 3D printing system, unlike Delta-type printers, the movement system used was Cartesian, as it is easier to program and because it is the most used in 3D printers made of polymeric material. However, unlike these printers, the print head is fixed in the 3 axes, with the printing table being responsible for all movement.

PROCEDURE

The ceramic mass used was sodium faience, sold by the company CERMASSA / PASTACER (Campo Largo / PR), with a firing temperature of 1,130ºC, total shrinkage of 10% and water absorption of 13%. These specifications were provided by the manufacturer and refer to the batch of product available.

For use in the project, the ground faience was dried at 60°C, passed through a sieve with a 0.425 mm mesh opening, hydrated with distilled and deionized water. The solid concentration of the mass was 73%. Finally, the mass was homogenized manually. To ensure that the composition always had the same plasticity, the Pfefferkorn Plasticimeter test was carried out to check whether it had suitable characteristics for extrusion, with this parameter being set between 3.0 and 3.5.

After printing, the pieces were dried for 24 hours at 60°C and fired for 2 hours at 1,130oC, at a heating rate of 10°C/min.

EXTRUSION 3D PRINTING DEVICE

To adjust the parameters for printing the dough, it was necessary to build the feeding system and the 3D moving system adapted to the universal testing machine (EMIC, DL10.000), the details of which were done by the authors in a previous publication [20] and are presented in Figure 2.

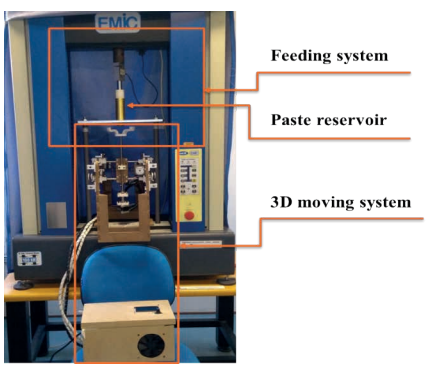

Figure 2: Assembled system for printing ceramic mass

FEEDING SYSTEM

Vertical bars, a horizontal plate and the piston and reservoir assembly were attached to the universal testing machine. The extrusion nozzle used is 20 mm long and 2 mm in diameter. The extrusion of the dough was controlled by the machine's TESC software, which is capable of varying the plunger speed between 0.02 and 500 mm/

min. For each test, the piston displacement speed was kept constant and the force required to extrude the dough was recorded. According to the principle of conservation of mass and considering the incompressible fluid, the extrusion speed is given by Equation (A), being: v_e: extrusion speed; D_{em}: plunger diameter; v_{em}: piston travel speed, and; D: print nozzle diameter.

$$v_e = \frac{D_{em}^2 . v_{em}}{D^2} \qquad (A)$$

For the tests, ceramic mass extrusion speeds of 10 to 12 mm/s were used, that is, it was necessary for the piston displacement speed to vary in the range of 1.872 to 2.247 mm/min.

3D MOVING SYSTEM

The 3D moving system 3D was built using laser-cut MDF parts and parts printed in PLA (polylactic acid). The fastening elements, displacement elements and electronic components for motion control are all commercially available.

The software used was Repetier-Host, which allows importing one or more 3D models, positioning, copying or changing the scale easily and allowing preview of the 3D printing [21, 22]. This software also has the function of manually controlling the printer, in addition to sending the script for printing written in G-Code, which defines the execution of the printhead path.

The speed of movement of the printing table was set at 10 mm/s, and the relationship between this and the extrusion speeds was investigated through visual inspection, by the appearance of stretches or, by excess material, in the printed test object. After printing, the specimens were qualitatively evaluated after drying and burning.

PRINT TEST

In all printing tests, when the path was changed, and consequently the G-Code sent to the printer, a test was carried out to check if the path was correct. This analysis was necessary because the codes were written manually, without the use of software capable of automatically generating them from a drawing. The result of this test for 2D tests can be seen in the image on the left in Figure 3, in which the defined path was 100 mm long, 60 mm wide, with a distance between the lines equal to the diameter of the nozzle (to result in in a theoretically solid specimen). For the 3D printing test, 3 printing layers were established, all with a length of 100 m and a width of 30 mm. An important consideration is the fact that the feeding system is continuous and that the beginning of the next layer must coincide with the end of the previous one. The image on the right in Figure 3 illustrates the beginning, end and connections between each of the layers, which present variations in direction to enable gains in mechanical resistance to the printed part.

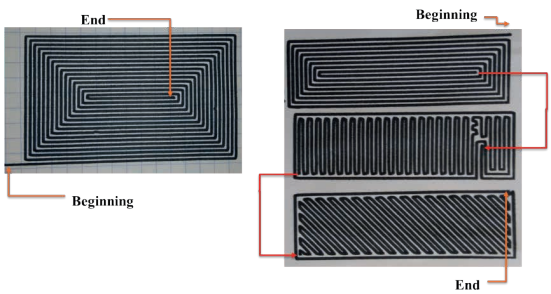

Figure 3: 2D left and 3D right test path

When printing samples with defined geometry in 3D, overlapping layers of ceramic material were printed on the Z axis, using displacement. Only the best conditions found in the 2D Tests were tested. It was also defined that, in all layers, the outer wall of the sample must be continuous, to finish the pieces. At this stage, there were no problems

identified, as the trajectories were correct and in accordance with the schedule, respecting maximum sizes and distance between lines.

2D PRINTING

Figure 4 shows in detail the ceramic mass being extruded on the table, without compressing the mass. The formats of the samples immediately after printing can be seen in Table 1, with each one representing the best result obtained for one of the tests, as specified in Table 1.

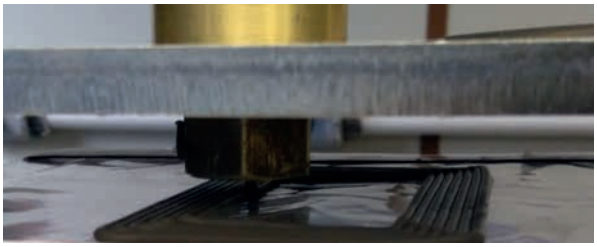

Figure 4: Detail of dough extrusion

Identification	Test	Difference in speeds	Number of test specimens	Print quality
A	Ve = Vm	0%	3	Bad
B	Ve = 1,05 * Vm	5%	4	Satisfactory
C	Ve = 1,10 * Vm	10%	3	Good
D	Ve = 1,15 * Vm	15%	3	Good
E	Ve = 1,20 * Vm	20%	2	Bad

Table 1: Number of 2D specimens

Comparing the results, it was possible to observe that by increasing the speed difference there was an improvement in the filling and execution of the edges of the test piece, as well as smaller deviations in the trajectory, due to the abrupt and specific variation in the extrusion speed. These gains were possible up to a 15% difference in speeds. In Figure 12-E there was excessive accumulation of material in the center and in the 90º angle corners of the samples. Qualitatively evaluating the results, Tests in condition C and D showed good filling of the corners, without any empty spaces and less deformation due to specific variations in extrusion speed.

According to Hu et al. [23], printing in which the layer height has a value close to the diameter of the extruder nozzle is the worst condition for density, porosity, shrinkage after sintering and mechanical resistance, as it results in low contact between layers. The ideal mathematical relationship between the extrusion speed and the table speed found by the authors for the case under study would be 3.5, which is greater than the 1.5 observed in the experiment.

During the drying stage, it was possible to observe the shrinkage of the specimens, which caused warping. This defect remained after the test specimens were burned, which increased flaws and voids, especially at the corners. Figure 5 illustrates these changes in detail.

Drying has two stages, in the first, the loss of water is accompanied by volumetric shrinkage, while in the second there is no shrinkage. Thus, according to Ghazanfari et al. [24], when the speed of water evaporation from the paste on the surface is greater than the mass transport, a pressure gradient occurs that leads to warping. Therefore, more controlled drying at a lower speed would reduce this effect.

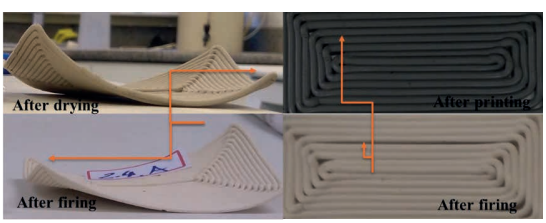

Figure 5: Change in the test specimen after drying and burning

After burning, the piece gains mechanical resistance and becomes easier to manipulate. It is possible to verify that after burning there

	After printing	After drying	After firing
A			
B		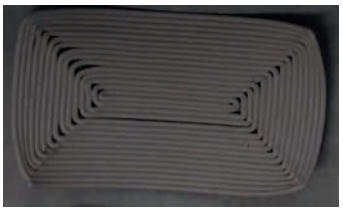	
C		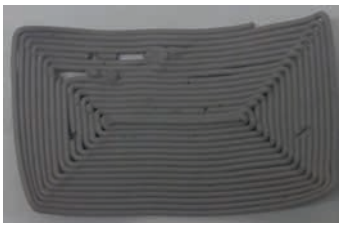	
D		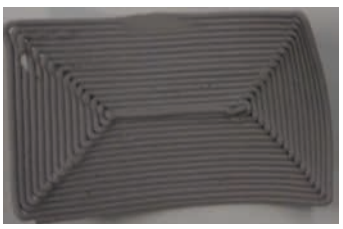	
E		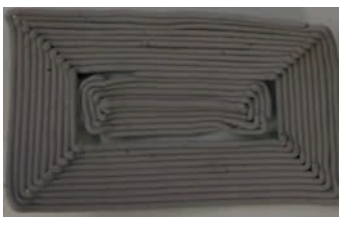	

Table 1: 2D test specimens after printing, drying and burning defined in Table 1

	Test A		Test B		Test C		Test D		Test E	
	D (mm)	F (N)	D (mm)	F (N)	D (mm)	F (N)	D (mm)	F (N)	D (mm)	F (N)
Proportionality Limit	0,52	288	0,46	282	0,38	245	0,34	201	0,39	255
Maximum Point	8,93	450	7,68	553	10,07	591	12,01	567	11,41	620

Table 2: Average values of Displacement (D) and Force (F) in 2D Printing

was adhesion between the filaments, forming a rigid test body. However, before burning, after drying, the specimen is still very fragile and therefore care must be taken when handling it.

ANALYSIS OF EXTRUSION FORCES

During the 2D printing tests, with the help of EMIC's TESC data capture program, the values of the force exerted by the equipment on the piston were collected in order to maintain the displacement of the Z axis constant. Figure 6 shows the average force versus piston displacement curves, relative to Tests A, B, C, D and E, as shown in Table 1.

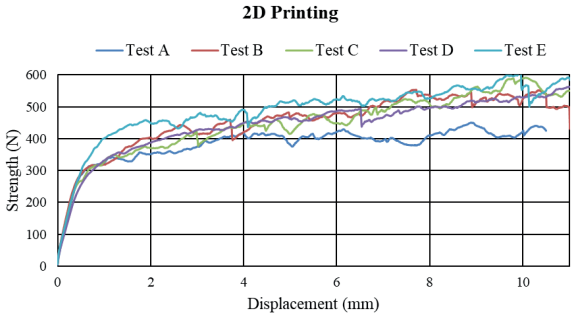

Figure 6: Force versus Displacement Curves in 2D Printing

It is possible to notice that initially the curves resemble a straight line with close angular coefficients overlapping each other. This condition is due to the fact that the material has the same consistency and plasticity. At the beginning of the flow there is an increase in the shear stress between the fluid and the reservoir wall. The proportionality limit is the last point of the initial linear part of the curve, which then presents an inflection and changes the slope. This stage is called yield limit, and from this point onwards the mass presents a permanent and fully developed flow. In this part of the curve, oscillations occur, which can be justified by the non-homogeneity of the mass, depending on the air contained inside. At these points, it was possible to verify during the tests that the oscillation in the flow sometimes occurred until the filament broke, generating discontinuity in the printing. Due to the oscillations, it was difficult to observe the yield point, thus determining the proportionality limit, Table 2.

It is possible to verify an increase in force between the proportionality limit and the maximum point (Table 2), that is, as the mass was compacted throughout the printing. This phenomenon occurs because the compression exerted by the plunger tends to exude water from the dough, and this phenomenon is observed in all Tests.

An increase in the average maximum force was noted as the extrusion speed increased, which was 22.9%, 31.3%, 26% and 37.8% in Tests B, C, D and E in relation to Test A, respectively.

In general terms, the variation in mass value between printing and drying was 25.3% and the total variation between printing and firing was 34%.

3D PRINTING

After qualitative analysis of the characteristics of the parts obtained in the 2D Tests, the parameters from Tests C and D were chosen to continue the 3D Test, from now on called Test F and G, respectively. In these two 3D printing tests, good filling of the corners was observed without excessive material deposition. The best results of the printed parts are shown in Figure 7.

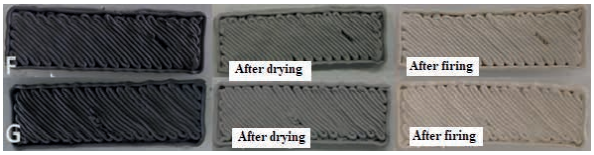

Figure 7: 3D specimens after printing, drying and burning

It is observed that, even though they are the best test specimens, there are air bubbles in the mass during filling of the layer, originating in Test F, which causes the extruded filament

to rupture and, consequently, filling failure. In Test G, the phenomenon is different. During the extrusion of the mass, in this specimen, there was an accumulation of material already at the exit of the nozzle that made up the specimen. It is observed that, for both tests, the final qualities of the specimens were satisfactory, and Test G, with a higher extrusion speed, presents a greater volume of deposited material, making the specimen more massive.

Another problem encountered when printing the test specimens was that, when executing curves, especially with very small angles, the mass itself hindered the printing, as shown in Figure 8, in which the path taken by the printer and the printing result are compared. According to Hergel et al. [25] curvature points with closed angles actually lead to material accumulation and defects that must be avoided when filling, it would have been better to choose a parallel contour filling strategy.

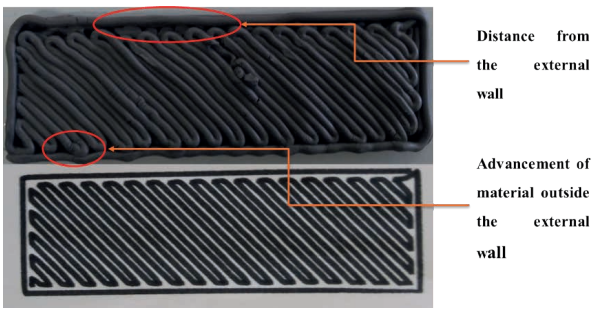

Figure 8: Test G 3D printed part defects

As a complement to the observation already made of the good interaction between filaments, in the same layer of printed material in the 2D Tests, in the 3D Tests this was even more noticeable. In Figure 9, it is possible to observe that, when depositing the filament that makes up the external wall of the second layer, deformation of the filament occurred in the form of waves in the contact region, due to the internal filament in the same layer. As highlighted by HU et al [23], due to the viscoelastic behavior of the clay paste, swelling of the extrudate occurs, which increases the diameter of the filament, contributing to these problems.

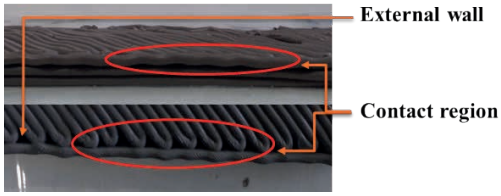

Figure 9: Adhesion of the ceramic material

During the drying stage it was possible to observe the same warping that occurred in the 2D Tests. This deformation was intensified after the bodies were burned. As can be seen in Figure 10 and already highlighted for the 2D Tests, Figure 5, the loss of water causes deformations and worsens existing ones. The difference occurs in the amplitude of the deformation, with 3D parts having less variation than 2D ones. In Figure 10 it is possible to verify the warping of the test specimens, a deformation that was verified in all tests carried out. It was still possible to notice that there was good adhesion between the layers. However, the edges in general were quite irregular, making it difficult to stack the layers in this region.

Figure 10: Warping of 3D Test Samples

ANALYSIS OF EXTRUSION FORCES

The force versus displacement graph curves of Tests F and G for 3D printing can be compared in Figure 11.

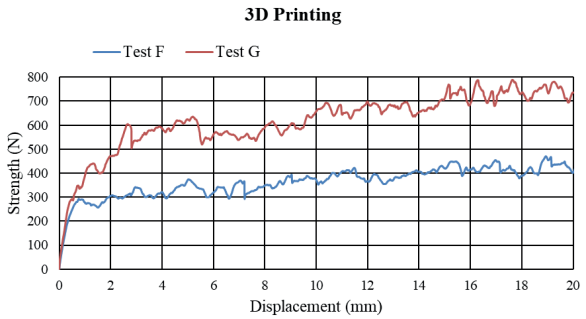

Figure 11: Force-Displacement Curves for Tests F and G

It is observed that the variation in force magnitude occurs when the extrusion speed of the ceramic mass is increased from 10 to 15% in relation to the table displacement speed. When analyzing the data from Tests F and G, a behavior similar to the data from Test C and D of 2D printing is observed, as can be seen in Table 3 by the proportionality limit and maximum force values found. This is as expected, since they present the same operating conditions.

	Test F		Test G	
	D (mm)	F (N)	D (mm)	F (N)
Proportionality Limit	0,38	250	0,35	259
Maximum Point	15,26	518	16,32	788

Table 3: Average values of Displacement (D) and Force (F) in 3D Printing

CONCLUSION

A 3D printing has already become widespread as an important facilitator for rapid prototyping, however the study of the behavior of ceramic mass with a high concentration of solids in extrusion printing has not yet been widely explored. To be able to better understand the process parameters of a ceramic plastic mass 3D printer, it is important to understand the factors that influence the printing characteristics. Therefore, the 3D printing device adapted to a universal testing machine can help in this process, by determining the force at which the fluid enters a steady state.

The present work consisted of testing a 3D printing device built by the authors, in addition to making programming adjustments, as the extrusion was continuous and without interruption. In the extrusion test, it was determined that the mass extrusion speed must be greater than the table displacement speed, in the range of 10% to 15%, providing this parameter with a significant improvement in printing quality. However, along with the increase in this speed, the forces necessary to carry out this extrusion also increase.

REFERENCES

[1] ALL ABOUT 3D PRINTING. Beginners Guide to Ceramic 3D Printing BEGINNER'S GUIDE TO 3D PRINTING. Disponível em < https://www.think3d.in/landing-pages/beginners-guide-to-3d-printing.pdf />. Acesso em: 03 nov. 2021.

[2] ISO/ASTM 52900: 2021 (en) Additive Manufacturing – General Principals – Fundamentals and Vocabulary.

[3] GIBSON, I.; ROSEN, D.; STUCKER, B. Additive Manufacturing Technologies 3D Printing, Rapid Prototyping, and Direct Digital Manufacturing. New York: Springer. 2nd. Ed., 2015.

[4] TRAVITZKY, N.; BONET, A; DERMEIK, B.; FEY, T.; FILBERT-DEMUT, I.; SCHLIER, L.; SCHLORDT, T.; GREIL, P. Additive Manufacturing of Ceramic-Based Materials. Advanced Engineering Materials, v. 16, n. 6, p. 729-754, 2014.

[5] BIKAS, H.; STAVROPOULOS, P.; CHRYSSOLOURIS, G. Additive manufacturing methods and modelling approaches: a critical review. **Int. J. Adv. Manuf. Technol**., v. 83, p. 389–405, 2016. DOI 10.1007/s00170-015-7576-2.

[6] LAKHDAR, Y.; TUCK, C.; BINNER, J.; TERRY, A.; GOODRIDGE, R. Additive manufacturing of advanced ceramic materials. **Progress in Materials Science,** 116, 2021. https://doi.org/10.1016/j.pmatsci.2020.100736.

[7] BLAZDELL, P.F.; EVANS, J.R.G. Application of a continuous ink jet printer to solid freeforming of ceramics. Journal of Materials Processing Technology, v. 99, p. 94-102, 2000.

[8] CHEN, H., ZHAO, Y. F. Process parameters optimization for improving surface quality and manufacturing accuracy of binder jetting additive manufacturing process. Rapid Prototyping Journal, v. 22, n. 3, p. 527-538, 2016.

[9] EXONE MATERIALS. **Industry Grade Materials**. Disponível em http://www.exone.com/Resources/Materials>. Acesso em: 05 nov. 2016.

[10] KUMAR, S.; KRUTH, J.-P. Composites by rapid prototyping technology. Materials & Design, v. 31, n. 2, p. 850-856, 2010.

[11] PALLERMO, E. What is Selective Laser Sintering? Disponível em <http://www.livescience.com/38862-selective-laser-sintering.html>. Acesso em: 04 nov. 2021

[12] SING, S. L.; YEONG, W. Y.; WIRIA, F. E.; TAY, B. Y.; TAY, B.Y.; ZHAO, Z.; ZHAO, L.; TIAN, Z.; YANG, S. Direct selective laser sintering and melting of ceramics: a review. Rapid Prototyping Journal, v. 23, n. 3, p. 611-623, 2017.

[13] REVELO, C. F.; COLORADO, H. A. 3D printing of kaolinite clay ceramics using the Direct Ink Writing (DIW) Technique. **Ceramics International**, v. 44, p.5673–5682, 2018.

[14] RUSCITTI, A.; TAPIA, C.; RENDTORFF, N. M. A review on additive manufacturing of ceramic materials based on extrusion processes of clay pastes**. Cerâmica,** v. 66, p**.** 354-366**,** 2020**.** http://dx.doi.org/10.1590/0366-69132020663802918**.**

[15] LIMA, P.; ZOCCA, A.; ACCHAR, W., GÜNSTER, J. 3D printing of porcelain by layerwise slurry deposition. **Journal of the European Ceramic Society**, v. 38, p.3395–3400, 2018.

[16] RUESCHHOFF, L.; COSTAKIS, W.; MICHIE, M.; YOUNGBLOOD, J.; TRICE, R. Additive Manufacturing of Dense Ceramic Parts via Direct Ink Writing of Aqueous Alumina Suspensions. **Int. J. Appl. Ceram. Technol**., v. 13, n. 5, p. 821–830, 2016. DOI:10.1111/ijac.12557.

[17] CHEN, Z.; LI, Z.; LI, J.; LIU, C.; LAO, C.; FU, Y.; LIU, C.; LI, Y.; WANG, P.; HE, Y. 3D printing of ceramics: A review. **Journal of the European Ceramic Society,** v. 39 p. 661–687, 2019.

[18] ZOCCA, A; COLOMBO, P.; GOMES, C. M.; GÜNSTER, J. Additive manufacturing of ceramics: issues, potentialities, and opportunities. **J. Am. Ceram. Soc.**, 98, v.7, p. 1983–2001, 2015. DOI: 10.1111/jace.13700

[19] COSTA, E. C.; DUARTE, J. P.; BÁRTOLO, P. Additive manufacturing for ceramic production. Rapid Prototyping Journal, v. 23, · n.5, p · 954–963, 2017.

[20] SILVA, G. A. ; GNOATO, J. H. A.; ARAÚJO, M. S.; MORAES, V. P.; KRETSCHEK, D.; CERRI, J. A. Mesa de Deslocamento Triaxial Adaptada à Máquina Universal de Ensaios usada em Desenvolvimento de uma Massa Cerâmica para Impressão 3D In: Soluções em Engenharia Mecânica Edição 2018: Melhores trabalhos de conclusão de curso do ano de 2017.1 Ed. Porto Alegre: Simplíssimo Livros, 2018, v.1, p. 192-205.

[21] REPETIER. Repetier. Disponível em <https://www.repetier.com/>. Acesso em: 19 mar. 2021.

[22] REPRAP**. Repetier**. Disponível em <http://reprap.org/wiki/Repetier>. Acesso em: 19 mar. 2021.

[23] HU, F.; MIKOLAJCZYK, T.; PIMENOV, D.Y.; GUPTA, M.K. Extrusion-Based. 3D Printing of Ceramic Pastes: Mathematical Modeling and In Situ Shaping Retention Approach. Materials, v. 14, p. 1137, 2021. http://doi.org/10.3390/ ma14051137.

[24] GHAZANFARIa, A.; LI, W; LEU, M. C.; HILMASB, G. E. A novel freeform extrusion fabrication process for producing solid ceramic components with uniform layered radiation drying. Additive Manufacturing, v. 15, p. 102–112, 2017.

[25] HERGEL, J.; HINZ, K; LEFEBVRE, S.; THOMASZEWSKI B. Extrusion-Based Ceramics Printing with Strictly-Continuous DepositionACM Trans. Graph., v. 38, n. 6, Article 194, 2019.